THE JOURNAL OF PHYSICAL CHEMISTRY C

Article

pubs.acs.org/JPCC

Functionalization of Open Two-Dimensional Metal–Organic Templates through the Selective Incorporation of Metal Atoms

Jan Čechal,*[,†,⊥] Christopher S. Kley,[†] Takashi Kumagai,[†] Frank Schramm,[‡] Mario Ruben,[‡,§] Sebastian Stepanow,*[,†] and Klaus Kern[†,∥]

[†]Max-Planck-Institut für Festkörperforschung, Heisenbergstrasse 1, D-70569 Stuttgart, Germany

[‡]Institute of Nanotechnology, Karlsruhe Institute of Technology, D-76344 Eggenstein-Leopoldshafen, Germany

[§]IPCMS-CNRS UMR 7504, Université de Strasbourg, 23 Rue du Loess, F-67034 Strasbourg, France

[∥]Institut de Physique de la Matière Condensée, Ecole Polytechnique Fédérale de Lausanne, CH-1015 Lausanne, Switzerland

Supporting Information

ABSTRACT: Surface-confined molecular networks can serve as templates to steer the adsorption and organization of secondary ligands, metal atoms, and clusters. Here, the incorporation of Ni atoms and clusters into open two-dimensional robust metal–organic templates self-assembled from butadiyne dibenzoic acid molecules and Fe atoms on Au(111) and Ag(100) surfaces is investigated by scanning tunneling microscopy. The metal substrate plays a crucial role in the interaction of Ni atoms with the metal–organic host networks. On Ag(100) the metal–organic template steers the growth of Ni clusters underneath the network pattern near the central butadiyne moiety. In contrast, on Au(111) Ni interacts preferentially with the benzene rings forming size-limited clusters inside the network cavities. Thereby, on both surfaces Ni clusters consisting of a few atoms with both high areal density and thermal stability up to 450 K are realized. The Ni-functionalized networks enable the coordination of additional molecules into the open structures demonstrating the utilization of selective interactions for the assembly of multicomponent architectures at different organizational stages.

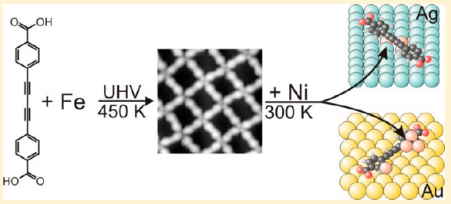

INTRODUCTION

The self-assembly protocols developed in the field of supramolecular chemistry are widely employed to engineer complex molecular architectures and materials with tailored properties.[1−9] In particular, bulk metal–organic frameworks (MOFs) and other porous compounds are highly versatile materials[8−12] that can be utilized, e.g., for gas storage[13] or heterogeneous catalysis.[14] Only recently, the interest has shifted also toward MOF films, thereby expanding and enhancing their applicability to membrane separators, chemical detectors, optical applications, and quartz crystal microbalance devices.[15,16] In the two-dimensional limit, metal–organic architectures as well as hydrogen-bonded networks confined to single-crystal metal surfaces have been intensively studied for gaining fundamental insights into the substrate governed self-assembly phenomena[17−19] as well as to investigate their potential in the fields of surface patterning,[20] catalysis,[21] and organic-based magnetism.[22]

Functionality in materials is often achieved by incorporating particular molecular or inorganic components into the framework that do not necessarily serve as building blocks in the primary structure. First, a robust framework and template is constructed with suitable lattice structure, porosity, and well-defined anchoring sites, followed by the incorporation of functional units at a higher organizational stage.[8,23−25] At surfaces, molecular networks were tested for their suitability to serve as host–guest systems[26] and as templates to steer the adsorption and organization of secondary ligands[20] and metal atoms and clusters.[27,28] However, the thermal stability of the latter proved to be challenging. Further, the metal decorated networks and templates have so far not been used to incorporate ligand molecules at a second stage of organization.

Here, we demonstrate the selective incorporation of Ni atoms and clusters into two-dimensional metal–organic templates on Ag(100) and Au(111) surfaces that allows to coordinate additional molecules into the open structure. The host coordination network self-assembles from bifunctional ligands (4,4′-di(1,4-buta-1,3-diynyl)benzoic acid (BDBA), Figure 1) and Fe atoms and provides a robust and flexible matrix.[29] Scanning tunneling microscopy (STM) reveals the selective interaction of Ni atoms with the Fe–BDBA network. Depending on the substrate, Ni atoms decorate either the benzene rings (Au) or the butadiyne moiety (Ag) of the ligand, while the network remains thermally stable up to 450 K. The

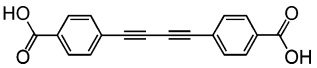

4,4'-di-(1,4-buta-1,3-diynyl)-benzoic acid

Figure 1. Molecular structure of the BDBA ligand.

Received: February 14, 2013
Revised: April 9, 2013
Published: April 23, 2013

   dx.doi.org/10.1021/jp4015977 | J. Phys. Chem. C 2013, 117, 8871−8877

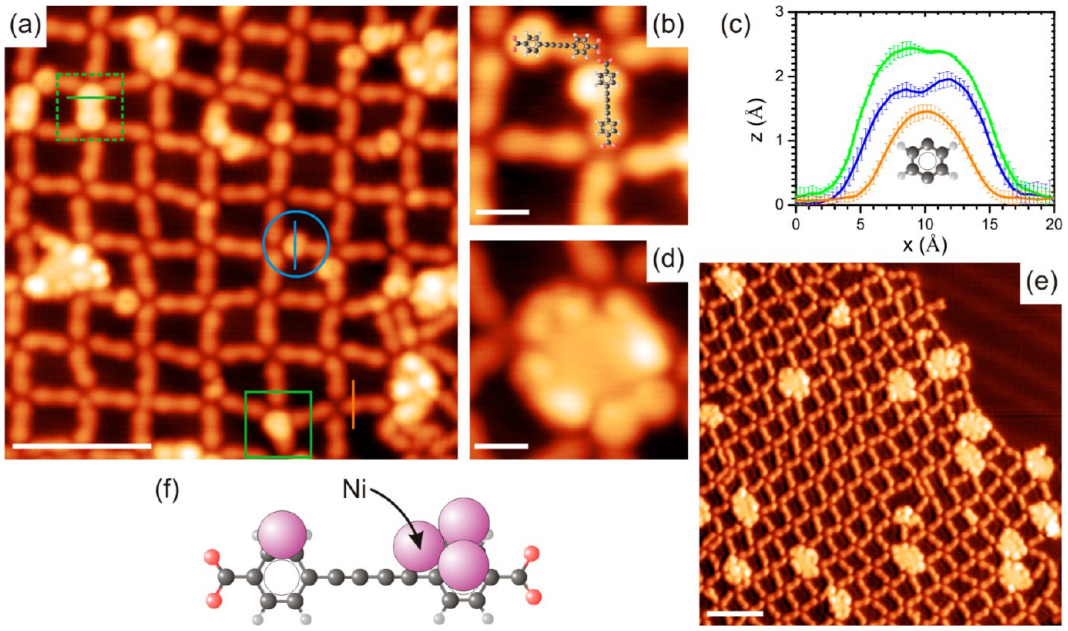

Figure 2. Representative STM images acquired after Ni deposition at 300 K on the Fe−BDBA network on Au(111). (a) Typical Ni-induced features near the benzene rings (blue circle, solid square) or entire BDBA (dotted square) are highlighted. (b) High-resolution image of the decorated benzene rings with superimposed BDBA model. (c) The average profiles (with 1σ error bars) corresponding to the line colors in (a). (d) High-resolution image of a filled cavity. (e) Upon annealing to 385 K only the filled cavities remain. (f) Model of possible binding sites of the Ni atoms to BDBA. Acquisition parameters: 5 K, 1 nA, −0.2 V (a, b) and 5 K, 1 nA, +0.5 V (d, e). Scale bars: 5 nm (a, e) and 1 nm (b, d).

striking difference in the Ni binding behavior reveals that besides selective Ni−ligand interactions also the substrate-dependent Ni atom diffusion processes play a role in the network functionalization. The incorporation of additional ligands into the network cavities coordinating to Ni atoms enables the assembly of robust architectures at different organizational stages.

EXPERIMENTAL METHODS

All experiments have been carried out in two separate UHV chambers (base pressure ~2 × 10^{-8} Pa) hosting a homemade variable-temperature STM and a low-temperature STM (5 K) and standard tools for preparation of well-defined metal surfaces.

Clean Ag(100) and Au(111) surfaces were prepared by cycles of Ar^+ sputtering and annealing to 800 K, followed by a slow substrate cooling to room temperature. The metal−organic networks were prepared by simultaneous deposition of Fe atoms and BDBA molecules on the substrate held at 450 K.[29] The BDBA molecules were deposited by thermal evaporation from a quartz crucible held at the temperature of 560 K and metal atoms using a standard e-beam evaporator (Omicron EFM3) at a flux current of 1 nA. During the deposition (5−15 min) the pressure was lower than 2 × 10^{-7} Pa. Ni atoms were deposited by a second e-beam evaporator on the substrate held at room temperature (300−305 K). The samples were then directly transferred to the respective STM.

The STM images were acquired either at room temperature or 5 K using electrochemically etched tungsten tips with a sample bias in the range from −1.0 to +1.2 V and tunneling currents ranging from 0.06 to 1.0 nA.

For the synthesis of the BDBA ligand we refer to ref 29.

RESULTS

Recently, we have demonstrated the formation of extended Fe−BDBA coordination networks on both Ag(100) and Au(111) surfaces, showing a high degree of structural flexibility and adaptability. The preparation and the properties of these networks are described in detail in ref 29. In brief, Fe adatoms and BDBA ligands form fully reticulated networks on Ag(100) and Au(111), in which Fe dimers coordinate to the carboxylate groups of four BDBA ligands. The rectangular arrays show the ability to adapt to surface defects and extend over multiple surface terraces exhibiting a high robustness and structural integrity of the network. The findings are ascribed to the high flexibility of the central BDBA butadiyne moiety. Further, the iron atoms interact exclusively with the carboxylate oxygen atoms leaving the butadiyne moiety virtually free, which serves as anchoring sites for transition metal atoms with high π-electron affinity, e.g., Ni. The Ni atoms can be utilized to bind additional ligands and functional units to the host network. Further, low-valent Ni atoms are potential active sites for CO_2 conversion.[30]

Ni Decoration of Fe−BDBA on Au(111). Figure 2 presents STM images of the Fe−BDBA network on Au(111) after subsequent nickel deposition at room temperature followed by cooling to 5 K. The BDBA ligands appear as dumbbell-like protrusions with an apparent height of 1.51 ± 0.04 Å at the benzene ring and 1.31 ± 0.04 Å at the center of the molecule, which is independent of the applied bias voltages (from −1.0 to +1.2 V). Upon Ni deposition the following features are identified in the STM images: (1) decoration of the benzene rings and (2) partial or complete filling of the network cavities.

The blue circle in Figure 2a marks a small protrusion at the benzene rings with an apparent height in the range 1.9−2.1 Å. The high-resolution image depicted in Figure 2b and the averaged line profile (blue) in Figure 2c reveal a small

dx.doi.org/10.1021/jp4015977 | J. Phys. Chem. C 2013, 117, 8871−8877

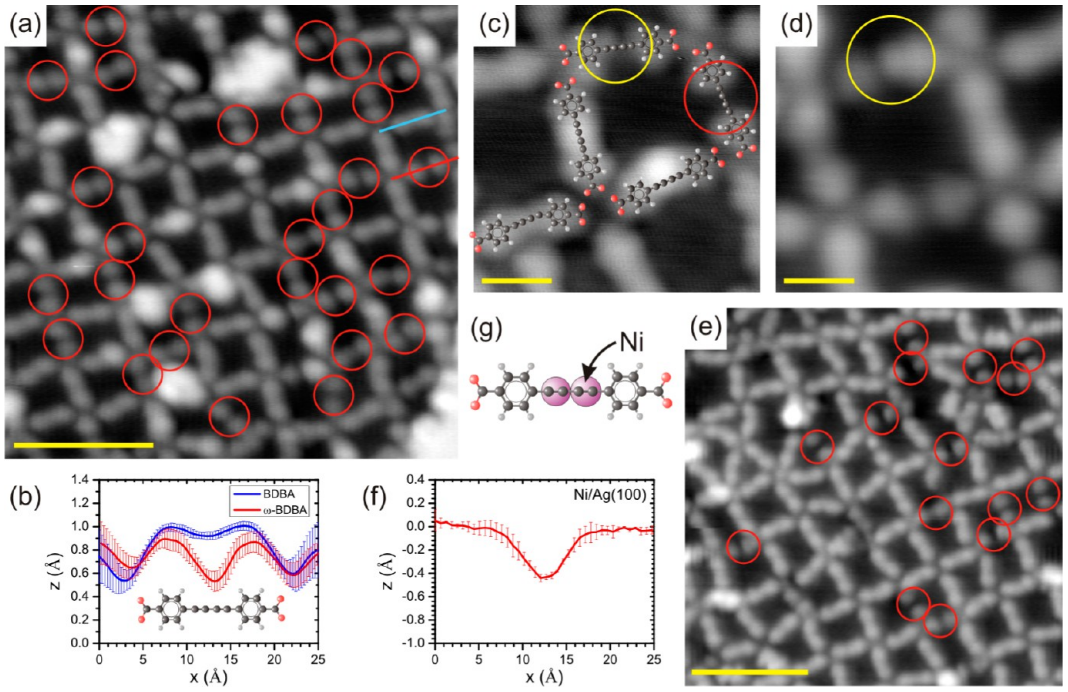

Figure 3. STM topographs of a Fe−BDBA/Ag(100) coordination network after Ni deposition at room temperature (a, c, and d) and after subsequent annealing to 450 K (e). (a) Red circles mark BDBA ligands with a pronounced depression at their centers (ω-BDBA). (b) Average profiles of pristine and ω-BDBA marked by color-coded lines in (a) with 1σ error bars. The magnified images (c) and (d) show the observed features in greater detail with the superimposed molecule model. (e) Only the ω-BDBA features remain after annealing to 450 K. (f) Line profile of a Ni atom embedded in the first Ag substrate layer. (g) Proposed trapping site of Ni atoms underneath the ligand molecules. Acquisition parameters: 5 K, 1 nA, +0.5 V (a, e), +0.7 V (c), and +0.2 V (d). Scale bars: 5 nm (a, e), and 1 nm (c, d).

asymmetry with respect to the long axis of the ligand. The somewhat larger features (marked by a green square in Figure 2a) have an apparent height of 2.2−2.5 Å, and their appearance extends from the benzene ring further to the center or over the entire molecule. The corresponding line profile (green) is shown in Figure 2c. We attribute all of these analyzed features to the presence of Ni atoms and small clusters which bind to the organic backbone of the network (see below).

Figure 2d shows a high-resolution image of a filled cavity, which apparent height of 2.0−2.6 Å at the center is close to the apparent height of Ni clusters on the bare Au(111). The position of the filled cavities correlates with the elbow sites of the herringbone reconstruction, which remains intact under the network (see Supporting Information for details).

Annealing to 385 K leads to the removal of the small features at the organic backbone, and only completely filled cavities remain within the networks (Figure 2e). After this treatment, the filled cavity interior shows a uniform height that corresponds to the formation of Ni islands with a height of monatomic Ni layer (2.1−2.4 Å).

Ni Decoration of Fe−BDBA on Ag(100). The incorporation of Ni atoms into the Fe−BDBA network on Ag(100) after deposition at room temperature followed by sample cooling to 5 K is illustrated in Figure 3. The apparent height of the pristine BDBA ligand on the Ag(100) surface is 1.01 ± 0.01 Å at the benzene ring and 0.93 ± 0.01 Å at the center. The following changes upon Ni deposition are observed: (1) lowering of the central part of the BDBA molecule, (2) appearance of protrusions near the ligands, and (3) filling of the network cavities.

The red circles in Figure 3a mark a large fraction of BDBA molecules (termed ω-BDBA) that display a bias-independent apparent height of 0.88 ± 0.07 Å at the benzene ring and 0.53 ± 0.05 Å at the central part of the ligand. The corresponding averaged line profiles are plotted in Figure 3b. The variation of the ω-BDBA profile is considerably larger compared to the pristine ligand, suggesting that a range of distinct configurations contribute to the appearance of the ω-BDBA molecules. The high-resolution images presented in Figure 3c,d reveal that some of the BDBA molecules display an asymmetry along the long axis with one benzene ring being lower than the other. Further, the apparent height at the center of the molecules can be as low as 0 Å. We attribute the dark features to Ni atoms residing underneath the molecules (see below).

Figure 3a shows additional relatively large protrusions with measured heights in the range of 1.4−2.2 Å that are tentatively attributed to metal clusters. These features are predominantly located near the central part of the ligands, and only a minority of clusters is found near the benzene rings. Also on Ag(100) some of the network cavities are completely filled with an apparent height of 2.05 Å that matches exactly the Ag substrate step height. As will be discussed below, both clusters and islands are composed of Ag atoms. Apart from the decoration of the network, rectangular metal ad-islands were found on the bare Ag surface (see Supporting Informmation for details).

Annealing to 385 K leads to a reduced amount of clusters decorating the network and an accompanied increase in the size of the metal ad-islands on the bare surface. Further annealing to 450 K removes nearly all cluster features inside the network with only ω-BDBA features remaining at the same abundance (Figure 3e).

Binding Guest Molecules into Ni-Functionalized Cavities on Ag(100). The applicability of the Ni-functionalized Fe−BDBA/Ag(100) networks for the hierarchical

dx.doi.org/10.1021/jp4015977 | J. Phys. Chem. C 2013, 117, 8871−8877

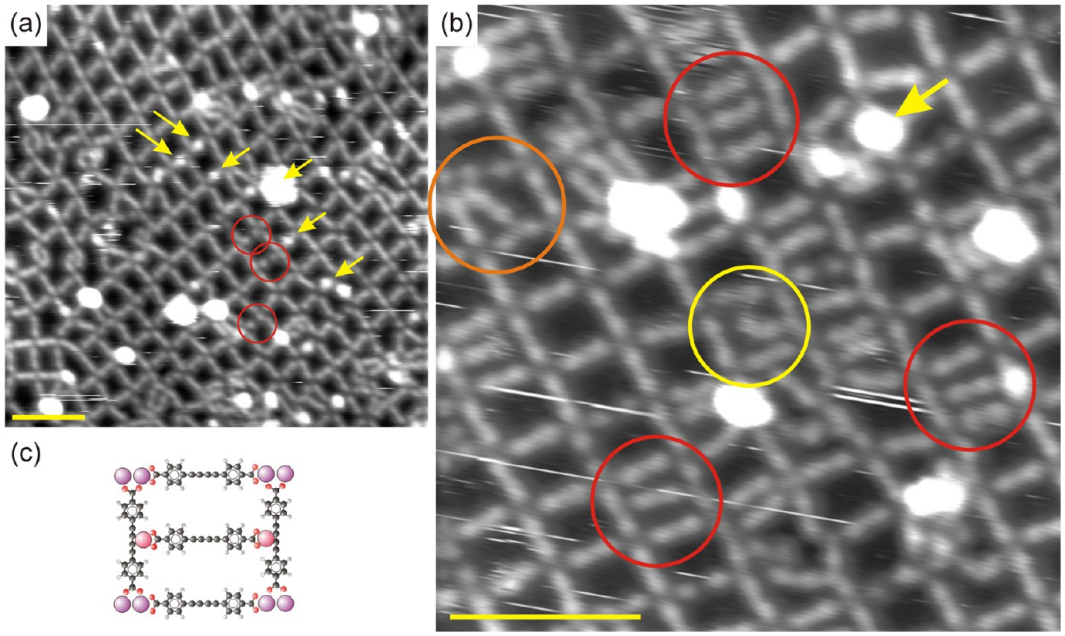

Figure 4. (a) STM image taken at room temperature shows the Ni-decorated Fe−BDBA/Ag(100) network before the deposition of additional BDBA molecules; the main features—ω-BDBA molecules and Ag clusters—are highlighted by red circles and yellow arrows, respectively. (b) Upon BDBA deposition (310 K), the additional BDBA molecules are bound into the cavities as highlighted by circles. The orange and yellow circles highlight accommodated BDBA molecules that point to a network node or to the center of a cavity molecule involving the bending of the guest molecule, respectively. Note that the Ag clusters are still present as marked by an arrow. (c) Tentative model of the BDBA bound into the cavity. Acquisition parameters: 300 K, 0.07 nA, −1.0 V (a) and 0.09 nA, −0.9 V (b). Scale bars: 5 nm.

assembly of multicomponent architectures is demonstrated by binding additional BDBA molecules into the cavities. Upon subsequent deposition of BDBA onto the Ni-decorated networks at room temperature (see Figure 4a), the molecules are bound into the cavities as depicted in Figure 4b. The guest BDBA molecule binds predominantly to the central butadiyne groups at the opposite sides of the cavity (see red circles in Figure 4b and scheme in Figure 4c). The accommodated BDBA molecules can also point to a network node or to the center of adjacent ligands of the cavity involving the bending of the guest molecule (marked by orange and yellow circles in Figure 4b, respectively). For steric reasons the ligands preferentially arrange parallel to the long side of the cavity. The accommodation of additional molecules was not observed for the plain Fe−BDBA network.

DISCUSSION

A number of distinct explanations for the nature and positions of the observed adspecies can be presented since a delicate interplay of a variety of mutual interactions and surface-related processes contributes to the resulting structure. On the bare substrate the surface diffusion and island nucleation may be altered by the interchange of incoming Ni metal atoms with atoms from first substrate layer (see Supporting Information for details). Besides reactive sites related to the substrate, e.g., step edges and heteroatoms embedded in substrate, the molecular networks, i.e., butadiyne group, phenyl rings, and coordination nodes, additionally modify the adatom diffusion. Moreover, the observed features are not necessarily the thermodynamically most stable ones because all above-mentioned processes are thermally activated. All these processes should be taken into account in order to reach a coherent and consistent interpretation of the experimental results. We start the discussion by considering the surface diffusion processes of Ni adatoms on the surfaces.

The distinct observations in the incorporation of Ni into the networks on the Au(111) and Ag(100) substrates can be understood by taking into account also the elementary processes for Ni atoms on the bare surfaces. On the Ag surface, Ni atoms exchange with the substrate atoms, assuming their thermodynamically most stable position within the first layer.[31,32] The associated activation energy amounts to only ∼0.3 eV,[33] enabling the exchange process even at low temperatures (∼130 K).[32] The surface diffusion of Ni atoms proceeds via an exchange diffusion mechanism within the topmost Ag layer[34] that can be assisted by Ag adatoms (from the exchange process) binding to the embedded Ni atom (Ni−Ag pair).[31] Ni atoms migrate in the first substrate layer and form islands,[35] following the standard nucleation and island growth model.[36]

The situation changes by the presence of the Fe−BDBA network on top of the surface. Here, the mobility of the Ni−Ag pair is spatially limited to the network cavity. The apparent depth of ∼0.4 Å associated with a single Ni atom (see exemplary profile in Figure 3f and Supporting Information for details) matches closely the lowering of the central part of the ω-BDBA molecules. Since no excessive segregation of Ni-related islands was observed on the bare surface, and no features were found within the exposed surface area of the cavities, we propose that the Ni atoms reside directly below the butadiyne group. During the diffusion process the Ni atoms are attracted by the high electron density of the alkynyl group, thereby breaking the Ni−Ag pair. Already a weak Ni−butadiyne attraction raises the diffusion barrier for the Ni atoms, which increases the residence time of the Ni atoms in the vicinity of the butadiyne moiety and consequently enhances the probability to form a stable nucleus by trapping a second Ni

dx.doi.org/10.1021/jp4015977 | J. Phys. Chem. C 2013, 117, 8871−8877

atom. Figure 3g illustrates the proposed geometry of the Ni nucleus. Its stability is enhanced by the absence of Ag adatoms assisting the Ni diffusion. The differences and variations in the measured heights of the ligands are thus ascribed to the number and geometry of Ni atoms below the molecules. In the proposed configuration, the Ni atoms could not be incorporated oxidatively by rehybridization of the alkynyl bonds since this would lead to a strong upward bending of the ligand.[37−41] Therefore, we expect a rather weak nonoxidative binding between Ni and BDBA.[42,43]

To accommodate the additional BDBA into the cavity as shown in Figure 4b, we presume that the Ni atom is lifted again above the surface. The energy gain from the formation of coordination bonds (∼1.2 eV)[44] is much higher than the energy expense (∼0.4 eV) needed for lifting the embedded Ni atom.

Apart from the butadiyne moiety, the benzene rings also possess π-electron density, and the Ni atoms can be localized there. The benzene rings show a decrease in the apparent height of 0.13 ± 0.08 Å for the ω-BDBA ligands, which suggests the presence of Ni atoms below the aromatic rings. However, a reduced height of the benzene rings was always accompanied by a significantly lowered central part of the molecules. Thus, we infer that the presence of Ni atoms under the aromatic rings is a result of the continuing growth of the Ni clusters and that the benzene rings do not serve as primary nucleation sites.

The stability of the Ni functionalized network at temperatures exceeding 450 K is significantly higher compared to previous reports, in which Co and Fe decorated networks start to collapse above 250 K.[27] Since every molecule in the network acts as a nucleation site for Ni atoms, the resulting pattern shows a mean Ni cluster distance of 2 nm corresponding to an areal density of 4×10^{13} clusters/cm^2. Besides the organic templates,[27,28] other patterning methods can be employed to steer the cluster growth with comparable areal cluster density. These include the use of surface strain relief patterns,[45] surface oxide templates,[46,47] or graphene Moiré patterns.[48] However, only the last two approaches also show appreciable cluster stability above room temperature.[47,48]

The trapped Ni atoms and clusters can serve as a template for the growth of metal clusters of a third kind as demonstrated by the presence of Ag clusters. These Ag adatoms originate from the Ni−Ag exchange process and aggregate close to embedded Ni atoms inside the networks or on the bare surface. The room temperature stability of the Ag clusters is traced back to their appreciable binding energy of 0.59 eV in the vicinity of an embedded Ni atom. This energy gain increases to 0.82 eV for Ag adatoms in contact with two Ni atoms, which usually leads to the capping or encapsulating of Ni islands on the bare Ag surface.[31,35] At elevated temperatures, the Ag atoms can overcome the binding energy, resulting in the removal of the Ag clusters from the network area and to the attachment of the adatoms to the substrate step edges and Ag islands on the bare surface (Figure 3e).

In contrast to Ag(100), on the Au(111) surface the Ni adatom interchange takes place only in the vicinity of elbow sites of the herringbone reconstruction,[49] leading to the preferential formation of Ni islands at these sites.[50,51] This preference is maintained even within the network area. However, the size of the clusters is limited to the size of the cavity. The composition of these islands is presumably a mixture of Ni and Au atoms.[52]

On Au(111) the Ni atoms show only a low affinity to the butadiyne moiety but rather interact more strongly with the benzene rings. The interaction of transition metal atoms with the benzene rings of organic templates was reported recently. Cobalt atoms residing on top of the benzene rings were observed for both coordination networks[27] and molecular adlayers[28] on a Ag(111) substrate. The observations were explained by the formation of stable half-sandwich complexes.[53] Similar behavior was observed for Fe atoms decorating the benzene rings at lower temperatures (90−130 K).[27] In this work a slightly asymmetric binding of the Ni atoms to the benzene rings was found on Au(111) (cf. Figures 2b and 2c). The calculated binding energy to a free benzene ring is considerably lower for Ni (1.73 eV) compared to Co (2.58 eV).[54] On the other hand, the adsorption energy of a Ni adatom on Au(111) amounts to about 2.9 eV.[44] Hence, a preferential binding of Ni atoms to the substrate would be expected. This explains the observation of filled cavities after annealing the substrate, which was not observed for both Fe and Co atoms on the Ag(111) surfaces.[27] The Ni binding to the benzene rings is only metastable for the BDBA ligands on Au(111).

Further insight into the selective interaction of Ni atoms with the BDBA ligand on the two surfaces can be gained by the investigation of the Ni−BDBA interaction in the absence of Fe (see Supporting Information for further details). On Au(111), Ni binds almost exclusively to the carboxylate oxygen atoms, forming nearly identical network structures as Fe−BDBA. Contrarily, on Ag(100) predominantly disordered structures were found that involve the binding of Ni adatoms equally to the carboxylate and the butadiyne groups. The bonding to the latter is sufficiently strong to bend the ligands, indicating a strong oxidative Ni−butadiyne association.[37−41] However, for an existing Fe−BDBA network this strong binding is only possible at the network periphery, i.e., for undercoordinated ligands. Here, strong deformations of the BDBA molecules were observed even on the Au(111) surface. Within the network, the BDBA geometry is fixed by the dominant coordination bonds to Fe atoms, and hence, the structural change associated with the rehybridization of alkynyl bonds is not possible. Consequently, the Ni atoms can only interact nonoxidatively with the high π-electron density of the butadiyne group, which results in a much weaker binding of Ni atoms to the ligand molecules.

The striking difference in the behavior of the Ni binding on Au(111) and Ag(100), both to the free ligands and within the Fe-BDBA networks, highlights the role of the underlying substrate. On the one hand, the Ni adatom processes are distinct on the two surfaces as described above, and on the other hand, the specific interaction of the π-electrons of the butadiyne moiety and benzene rings with the metal substrates results in different chemical states of the constituents on the two surfaces and hence to different affinities to Ni atoms.

CONCLUSIONS

In summary, we have demonstrated the incorporation of Ni atoms and clusters into open two-dimensional robust metal−organic templates. The functionalized networks are thermally stable at temperatures up to 450 K and enable the coordination of additional molecules into the open structures, demonstrating the utilization of selective interactions for the assembly of multicomponent architectures at different organizational stages. Further, we showed that the employed metal substrate plays a

dx.doi.org/10.1021/jp4015977 | J. Phys. Chem. C 2013, 117, 8871−8877

crucial role in the interaction of transition metal atoms with the metal−organic host networks. On the Ag(100) substrate, the surface-confined metal−organic template steers the growth of the Ni clusters underneath the network pattern. Here, the embedded Ni atoms nucleate preferentially at the butadiyne moiety of the BDBA ligands. Thereby, Ni clusters consisting of a few metal atoms with an areal density of 4×10^{13} cm^{-2} can be obtained. In contrast, on the Au(111) substrate the Ni atoms interact preferentially with the BDBA benzene rings and form size-limited clusters inside the cavities.

The work demonstrates the unique occurrence of selective interactions in a multicomponent system including the surface that may be further explored to create functional molecular architectures with novel properties. Moreover, the stability and direct accessibility of the noncapped Ni atoms and clusters on both gold and silver substrates render these systems attractive candidates to explore their catalytic activity.

■ ASSOCIATED CONTENT

Ⓢ Supporting Information

(1) Ni clusters and cavity filling of the Fe−BDBA network on Au(111), (2) Ni deposition on the bare Ag(100) substrate, and (3) Ni−BDBA networks. This material is available free of charge via the Internet at http://pubs.acs.org.

■ AUTHOR INFORMATION

Corresponding Author

*Tel +420 541 142 810, e-mail cechal@fme.vutbr.cz (J.Č.); Tel +49 711 689 1541, e-mail s.stepanow@fkf.mpg.de (S.S.).

Present Address

⊥J.Č.: Institute of Physical Engineering and CEITEC, Brno University of Technology, Technická 2896/2, 616 69 Brno, Czech Republic.

Notes

The authors declare no competing financial interest.

■ ACKNOWLEDGMENTS

The work was supported by the Baden-Württemberg Stiftung. J.Č. acknowledges the support of a Marie Curie Intra European Fellowship within the 7th European Community Framework Programme (AdaptNano, Project No. 251930) and "CEITEC − Central European Institute of Technology" (CZ.1.05/1.1.00/02.0068) from the European Regional Development Fund. T.K. acknowledges support from the JSPS (Japan Society for the Promotion of Science).

■ REFERENCES

(1) Lehn, J. M. *Supramolecular Chemistry: Concepts and Perspectives*; Wiley-VCH: Weinheim, 1995.

(2) Rao, C. N. R.; Natarajan, S.; Vaidhyanathan, R. Metal carboxylates with open architectures. *Angew. Chem., Int. Ed.* **2004**, *43*, 1466−1496.

(3) Klemm, D.; Heublein, B.; Fink, H.-P.; Bohn, A. Cellulose: Fascinating biopolymer and sustainable raw material. *Angew. Chem., Int. Ed.* **2005**, *44*, 3358−3393.

(4) Wiester, M. J.; Ulmann, P. A.; Mirkin, C. A. Enzyme mimics based upon supramolecular coordination chemistry. *Angew. Chem., Int. Ed.* **2011**, *50*, 114−137.

(5) Kato, T.; Mizoshita, N.; Kishimoto, K. Functional liquid-crystalline assemblies: Self-organized soft materials. *Angew. Chem., Int. Ed.* **2006**, *45*, 38−68.

(6) Brammer, L. Developments in inorganic crystal engineering. *Chem. Soc. Rev.* **2004**, *33*, 476−489.

(7) Descalzo, A. B.; Martínez-Máñez, R.; Sancenón, F.; Hoffmann, K.; Rurack, K. The supramolecular chemistry of organic-inorganic hybrid materials. *Angew. Chem., Int. Ed.* **2006**, *45*, 5924−5948.

(8) Calzaferri, G.; Huber, S.; Maas, H.; Minkowski, C. Host-guest antenna materials. *Angew. Chem., Int. Ed.* **2003**, *42*, 3732−3758.

(9) Furukawa, H.; Ko, N.; Go, Y. B.; Aratani, N.; Choi, S. B.; Choi, E.; Yazaydin, A. Ö.; Snurr, R. Q.; O'Keeffe, M.; Kim, J.; Yaghi, O. M. Ultrahigh porosity in metal-organic frameworks. *Science* **2010**, *329*, 424−428.

(10) O'Keeffe, M.; Yaghi, O. M. Deconstructing the crystal structures of metal−organic frameworks and related materials into their underlying nets. *Chem. Rev.* **2012**, *112*, 675−702.

(11) Meek, S. T.; Greathouse, J. A.; Allendorf, M. D. Metal-organic frameworks: A rapidly growing class of versatile nanoporous materials. *Adv. Mater.* **2011**, *23*, 249−267.

(12) Meilikhov, M.; Yusenko, K.; Esken, D.; Turner, S.; van Tendeloo, G.; Fischer, R. A. Metals at MOFs − loading MOFs with metal nanoparticles for hybrid functions. *Eur. J. Inorg. Chem.* **2010**, *2010*, 3701−3714.

(13) Sumida, K.; Rogow, D. L.; Mason, J. A.; McDonald, T. M.; Bloch, E. D.; Herm, Z. R.; Bae, T.-H.; Long, J. R. Carbon dioxide capture in metal−organic frameworks. *Chem. Rev.* **2012**, *112*, 724−781.

(14) Yoon, M.; Srirambalaji, R.; Kim, K. Homochiral metal−organic frameworks for asymmetric heterogeneous catalysis. *Chem. Rev.* **2012**, *112*, 1196−1231.

(15) Shekhah, O.; Liu, J.; Fischer, R. A.; Wöll, Ch. MOF thin films: Existing and future applications. *Chem. Soc. Rev.* **2011**, *40*, 1081−1106.

(16) Betard, A.; Fischer, R. A. Metal−organic framework thin films: From fundamentals to applications. *Chem. Rev.* **2012**, *112*, 1055−1083.

(17) Bartels, L. Tailoring molecular layers at metal surfaces. *Nat. Chem.* **2010**, *2*, 87−95.

(18) Elemans, J. A. A. W.; Lei, S.; De Feyter, S. Molecular and supramolecular networks on surfaces: From two-dimensional crystal engineering to reactivity. *Angew. Chem., Int. Ed.* **2009**, *48*, 7298−7332.

(19) Lin, N.; Stepanow, S.; Ruben, M.; Barth, J. V. Surface-confined supramolecular coordination chemistry. *Top. Curr. Chem.* **2009**, *287*, 1−44.

(20) Madueno, R.; Räisänen, M. T.; Silien, C.; Buck, M. Functionalizing hydrogen-bonded surface networks with self-assembled monolayers. *Nature* **2008**, *454*, 618−621.

(21) Fabris, S.; Stepanow, S.; Lin, N.; Gambardella, P.; Dmitriev, A.; Honolka, J.; Baroni, S.; Kern, K. Oxygen dissociation by concerted action of di-iron centers in metal−organic coordination networks at surfaces: Modeling non-heme iron enzymes. *Nano Lett.* **2011**, *11*, 5414−5420.

(22) Gambardella, P.; Stepanow, S.; Dmitriev, A.; Honolka, J.; de Groot, F. M. F.; Lingenfelder, M.; Gupta, S. S.; Sarma, D. D.; Bencok, P.; Stanescu, S.; Clair, S.; Pons, S.; Lin, N.; Seitsonen, A. P.; Brune, H.; Barth, J. V.; Kern, K. Supramolecular control of the magnetic anisotropy in two-dimensional high-spin Fe arrays at a metal interface. *Nat. Mater.* **2009**, *8*, 189−193.

(23) Elemans, J. A. A. W.; Rowan, A. E.; Nolte, R. J. M. Mastering molecular matter. Supramolecular architectures by hierarchical self-assembly. *J. Mater. Chem.* **2003**, *13*, 2661−2670.

(24) Soler-Illia, G. J. de A. A.; Sanchez, C.; Lebeau, B.; Patarin, J. Chemical strategies to design textured materials: From microporous and mesoporous oxides to nanonetworks and hierarchical structures. *Chem. Rev.* **2002**, *102*, 4093−4138.

(25) Ikkala, O.; ten Brinke, G. Hierarchical self-assembly in polymeric complexes: Towards functional materials. *Chem. Commun.* **2004**, *2004*, 2131−2137.

(26) Cicoira, F.; Santato, C.; Rosei, F. Two-dimensional nano-templates as surface cues for the controlled assembly of organic molecules. *Top. Curr. Chem.* **2008**, *285*, 203−267.

(27) Decker, R.; Schlickum, U.; Klappenberger, F.; Zoppellaro, G.; Klyatskaya, S.; Ruben, M.; Barth, J. V.; Brune, H. Using metal-organic templates to steer the growth of Fe and Co nanoclusters. *Appl. Phys. Lett.* **2008**, *93*, 243102.

(28) Krenner, W.; Klappenberger, F.; Kuhne, D.; Diller, K.; Qu, Z.-R.; Ruben, M.; Barth, J. V. Positioning of single Co atoms steered by a self-assembled organic molecular template. *J. Phys. Chem. Lett.* **2011**, *2*, 1639−1645.
(29) Kley, C. S.; Cechal, J.; Kumagai, T.; Schramm, F.; Ruben, M.; Stepanow, S.; Kern, K. Highly adaptable two-dimensional metal-organic coordination networks on metal surfaces. *J. Am. Chem. Soc.* **2012**, *134*, 6072−6075.
(30) Cokoja, M.; Bruckmeier, C.; Rieger, B.; Herrmann, W. A.; Kuhn, F. E. Transformation of carbon dioxide with homogeneous transition-metal catalysts: A molecular solution to a global challenge? *Angew. Chem., Int. Ed.* **2011**, *50*, 8510−8537.
(31) Caffio, M.; Atrei, A.; Bardi, U.; Rovida, G. Growth mechanism and structure of nickel deposited on Ag(001). *Surf. Sci.* **2005**, *588*, 135−148.
(32) Langelaar, M. H.; Boerma, D. O. Fe adatoms on Ag(100): Site exchange and mobility. *Surf. Sci.* **1998**, *395*, 131−137.
(33) Perkins, L. S.; DePristo, A. E. Heterogeneous adatom diffusion on fcc(100) surfaces: Ni, Cu, Rh, Pd, and Ag. *Surf. Sci.* **1994**, *319*, 225−231.
(34) Canepa, M.; Terreni, S.; Cantini, C.; Campora, A.; Mattera, L. Initial growth morphology in a heteroepitaxial system at low temperature: Fe on Ag(100). *Phys. Rev. B* **1997**, *56*, 4233−4242.
(35) Hite, D. A.; Kizilkaya, O.; Sprunger, P. T.; Howard, M. M.; Ventrice, C. A., Jr.; Geisler, H.; Zehner, D. M. Surface morphology and electronic structure of Ni/Ag(100). *J. Vac. Sci. Technol. A* **2000**, *18*, 1950−1954.
(36) Venables, J. A.; Spiller, G. D. T.; Hanbucken, M. Nucleation and growth of thin films. *Rep. Prog. Phys.* **1984**, *47*, 399−459.
(37) Klettke, T.; Walther, D.; Schmidt, A.; Gorls, H.; Imhof, W.; Gunther, W. Synthesis, structure and reactions of the homoleptic alkyne nickel(0) complex $(alkyne)_4Ni_3$ (alkyne: 2-methyl-4-trimethyl-silyl-3-butyn-2-ol). *Chem. Ber.* **1996**, *129*, 1457−1461.
(38) Braga, D.; Grepioni, F.; Walther, D.; Heubach, K.; Schmidt, A.; Imhof, W.; Gorls, H.; Klettke, T. From alkynols to alkynol complexes. A molecular assembly study. *Organometallics* **1997**, *16*, 4910−4919.
(39) Hyla-Kryspin, I.; Koch, J.; Gleiter, R.; Klettke, T.; Walther, D. Reassessment of the electronic and molecular structure, bonding, and stability of zerovalent nickel acetylene complexes by the density functional method. *Organometallics* **1998**, *17*, 4724−4733.
(40) Walther, D.; Dohler, T.; Heubach, K.; Klobes, O.; Schweder, B.; Gorls, H. Catalytic cyclization and dimerization of 1.5-hexadiene by transition metals: The reactivity of NiII and PdII complexes containing bi- or tridendate ligands and of bis(alkyne)nickel(0) compounds. *Z. Anorg. Allg. Chem.* **1999**, *625*, 923−932.
(41) Koch, J.; Hyla-Kryspin, I.; Gleiter, R.; Klettke, T.; Walther, D. All-electron density functional study on electronic structure, stability, and Ni-Ni bonding in polynuclear nickel complexes with bridging alkyne ligands. *Organometallics* **1999**, *18*, 4942−4948.
(42) Bonrath, W.; Porschke, K. R.; Wilke, G.; Angermund, K.; Kruger, C. Mono- and dinuclear nickel(0) complexes of butadiyne. *Angew. Chem., Int. Ed. Engl.* **1988**, *27*, 833−835.
(43) Rosenthal, U.; Pulst, S.; Kempe, R.; Porschke, K.-R.; Goddard, R.; Proft, B. Pyridine-based mono(ligand)nickel(0) complexes of 1,6-heptadiene, 1-phenyl-2-trimethylsilylacetylene, and 1,4-bis-(trimethylsilyl)-1,3-butadiyne. *Tetrahedron* **1998**, *54*, 1277−1287.
(44) Clair, S.; Pons, S.; Fabris, S.; Baroni, S.; Brune, H.; Kern, K.; Barth, J. V. Monitoring two-dimensional coordination reactions: Directed assembly of co-terephthalate nanosystems on Au(111). *J. Phys. Chem. B* **2006**, *110*, 5627−5632.
(45) Brune, H.; Giovannini, M.; Bromann, K.; Kern, K. Self-organized growth of nanostructure arrays on strain-relief patterns. *Nature (London)* **1998**, *394*, 451−453.
(46) Schmid, M.; Kresse, G.; Buchsbaum, A.; Napetschnig, E.; Gritschneder, S.; Reichling, M.; Varga, P. Nanotemplate with holes: Ultrathin alumina on $Ni_3Al(111)$. *Phys. Rev. Lett.* **2007**, *99*, 196104.
(47) Becker, C.; Rosenhahn, A.; Wiltner, A.; von Bergmann, K.; Schneider, J.; Pervan, P.; Milun, M.; Kralj, M.; Wandelt, K. Al_2O_3-films on $Ni_3Al(111)$: A template for nanostructured cluster growth. *New J. Phys.* **2002**, *4*, 75.1−75.15.
(48) N'Diaye, A. T.; Bleikamp, S.; Feibelman, P. J.; Michely, T. Two-dimensional It cluster lattice on a graphene Moiré on Ir(111). *Phys. Rev. Lett.* **2006**, *97*, 215501.
(49) Meyer, J. A.; Baikie, I. D.; Kopatzki, E.; Behm, R. J. Preferential island nucleation at the elbows of the Au(111) herringbone reconstruction through place exchange. *Surf. Sci.* **1996**, *365*, L647−L651.
(50) Chambliss, D. D.; Wilson, R. J.; Chiang, S. Nucleation of ordered Ni island arrays on Au(111) by surface-lattice dislocations. *Phys. Rev. Lett.* **1991**, *66*, 1721−1724.
(51) Chambliss, D. D.; Wilson, R. J.; Chiang, S. Ordered nucleation of Ni and Au islands on Au(111) studied by scanning tunneling microscopy. *J. Vac. Sci. Technol. B* **1991**, *9*, 933.
(52) Cullen, W. G.; First, P. N. Island shapes and intermixing for submonolayer nickel on Au(111). *Surf. Sci.* **1999**, *420*, 53−64.
(53) Pandey, R.; Rao, B. K.; Jena, P.; Blanco, M. A. Electronic structure and properties of transition metal−benzene complexes. *J. Am. Chem. Soc.* **2001**, *123*, 3799−3808.
(54) BelBruno, J. J. Half-sandwich metal atom complexes with benzene: A model for adsorption onto graphite. *Surf. Sci.* **2005**, *577*, 167−174.